FIGURE 8. **Maturation of hypertrophic chondrocyte is impaired in metatarsals treated with FGF23/sKL.** A and B, metatarsal rudiments were isolated from E 15.5 embryos and cultured in the presence or absence of FGF23 (300 ng/ml) and sKL (300 ng/ml) for 6 days. Expression levels of Col10a1 were analyzed by In situ hybridization (A) and real-time-RT-PCR (B) (n = 3). C, primary chondrocytes were treated with chondrogenic media in the presence or absence of FGF23 (100 ng/ml) and sKL (100 ng/ml) for 6 days. Expression levels of Col10a1 were determined by real-time RT-PCR (n = 3). D and E, metatarsals were cultured in the presence of various concentrations of FGF23 and sKL (D), or FGF23 (300 ng/ml), sKL (300 ng/ml), or both (E) for 12 days. On day 12, the calcein incorporated area was visualized and quantified (n = 3–4). RZ: resting zone, PZ: proliferating zone, HZ: hypertrophic zone. The figures shown are the representative from at least three independent experiments. The values were expressed as mean ± S.E. *, $p < 0.01$; **, $p < 0.05$. ns, not significant.

ple, FGF23 has been recently shown to be responsible for the development of left ventricular hypertrophy through activating calcineurin-NFAT signaling pathway in mice (26). Non-canonical activity of FGF23 could be operative as well in chondrocytes as evidenced by the previous study in which Fgf23 and Slc34a1 genes were deleted in mice (10). The lack of Slc34a1 in Fgf23-deficient mice did not correct the decreased number of hypertrophic chondrocytes in Fgf23-deficient mice despite of the correction of serum phosphate levels, suggesting the presence of phosphate-independent action of FGF23 in chondrocytes; however, the precise mechanisms of phosphate-independent

function of FGF23 in chondrocyte biology remain to be elucidated.

Initially, we demonstrated in vitro that FGF23 can mediate its signals in the presence of sKL. As previously reported, α-Klotho expression was extremely low in chondrogenic cells. In line with this, FGF23 alone could not activate ERK or induce Egr1 expression in chondrogenic cells. Since there is an increasing amount of evidence that demonstrates the biological function of sKL in mice (12–15), we assessed the functional interaction between FGF23 and sKL in chondrogenic cells. In the current study, we utilized ~130 kDa of sKL produced by ectodomain
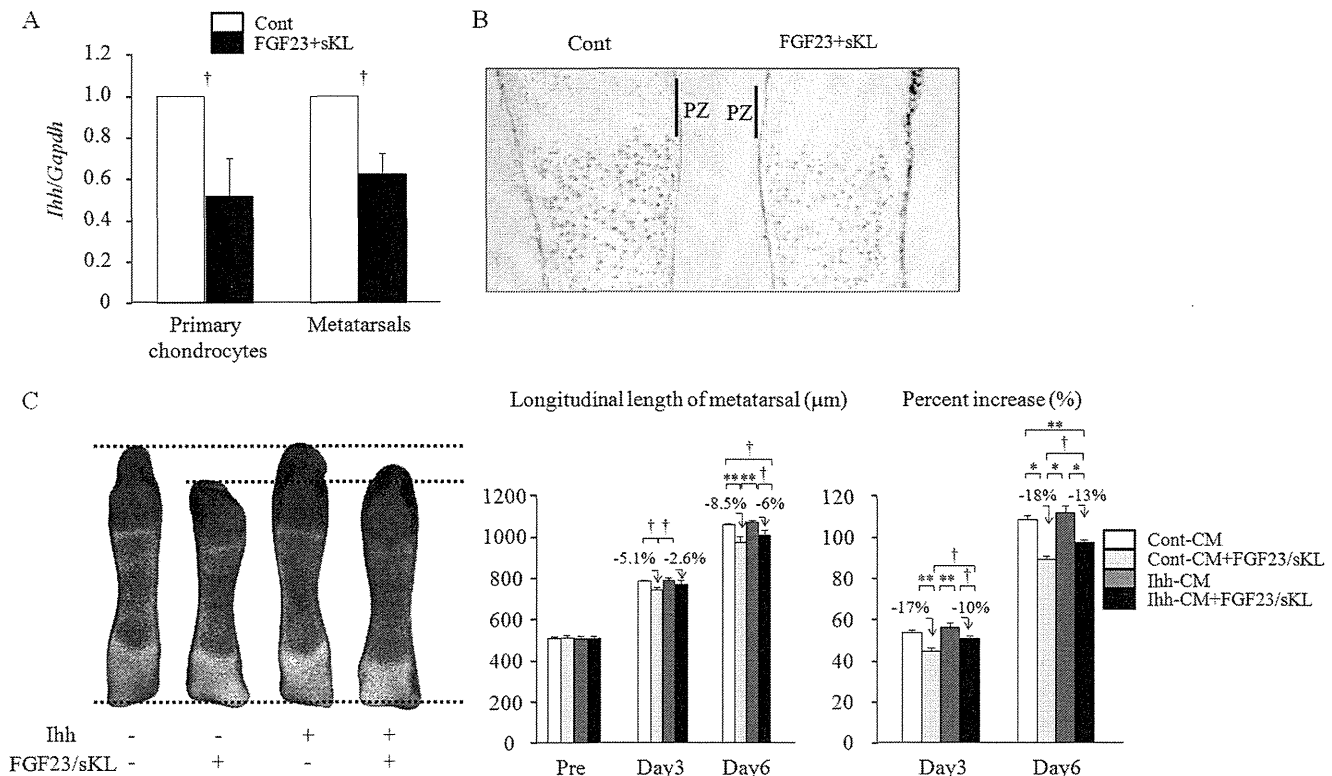
FIGURE 9. **Indian Hedgehog partly mediates the suppressive effect of FGF23/sKL on the longitudinal growth of metatarsals.** *A* and *B*, primary chondrocytes were treated with chondrogenic media in the presence or absence of FGF23 (100 ng/ml) and sKL (100 ng/ml) for 2 days. Metatarsal rudiments were cultured in the presence or absence of FGF23 (300 ng/ml) and sKL (300 ng/ml) for 6 days. Expression levels of *Ihh* were determined by real-time RT-PCR ($n = 4$) (*A*) and immunohistochemistry ($n = 3$) (*B*). *C*, metatarsals were treated with FGF23 (300 ng/ml) and sKL (300 ng/ml) for 6 days in the presence of 10% of Ihh conditioned media (Ihh-CM) or control conditioned media (Cont-CM) and longitudinal lengths and percent increases in metatarsals were measured ($n = 3-4$). Conditioned media obtained from HEK293 cells overexpressing empty vector were used as Cont-CM. *PZ*: proliferating zone. The figures shown are the representative from at least three independent experiments. The values were expressed as mean ± S.E. *, $p < 0.001$; **, $p < 0.01$; †, $p < 0.05$.

shedding based on a previous report showing that this type of sKL is the predominant sKL in human circulation (27). Interestingly, *in vitro* studies revealed that FGF23 exerted its signals in the presence of sKL in chondrogenic cells. The precise mechanisms whereby sKL mediates FGF23 signaling still need to be elucidated, but the finding that sKL forms a protein complex with FGF23 may raise the possibility that sKL may allow FGF23 to reach and bind to its specific receptors by making a complex with FGF23 in the circulation. Indeed, co-immunoprecipitation analysis revealed that the binding of FGF23 to FGFR3 was enhanced when sKL was present. However, it is still unclear as to whether FGF23/sKL complex is present in the circulation and further analyses are required to determine the significance of this complex in the *in vivo* physiological conditions.

Next, to elucidate the significance of FGF23/sKL signaling in chondrocyte biology, we introduced an *ex vivo* metatarsal organ culture system, which is a widely used procedure to recapitulate *in vivo* bone growth. Using this method, we found a unique phenotype with respect to chondrocyte proliferation such that FGF23/sKL suppressed proliferation in the proliferating zone. The finding that FGF23/sKL impaired chondrocyte proliferation in the proliferating zone led us to speculate that FGF23/sKL may recognize FGFR3 as its receptor because an activating mutation in the *Fgfr3* gene has been shown to result in impaired chondrocyte proliferation (28–30). Based on this, we analyzed whether FGFR3 is involved in FGF23/sKL-mediated suppression of metatarsal growth and provided evidence that FGFR3 is

at least in part involved in the FGF23/sKL-mediated action on metatarsal growth. However, given the fact that FGF23/sKL showed a non-significant suppression on the linear growth of metatarsals infected with adenovirus containing microRNA specific for *Fgfr3*, we could not exclude the possibility of the involvement of other types of FGF receptors, although it is still possible that residual expression of FGFR3 may contribute to the suppressive action in FGFR3-knocked down metatarsals. Similar to FGFR3, FGFR1 is abundantly expressed in the growth plate predominantly in perichondrium and hypertrophic chondrocytes, whereas FGFR3 exhibits abundant expression in resting and proliferating chondrocytes, with less expression in hypertrophic chondrocytes (31). The expression profile of FGFR2 is also different from FGFR3, and FGFR2 is mainly expressed in mesenchymal condensation (31). Although previous *in vitro* studies demonstrated the binding of FGF23 to multiple FGF receptors (8, 9), the compartment-specific expression profile of FGFRs in the growth plate would confer a specific binding partner for FGF23 in the presence of sKL such that FGF23 suppresses chondrocyte proliferation in the proliferating zone through the activation of FGFR3.

Multiple pathways have been shown to mediate the effect of FGFR3 activation with respect to the suppression of chondrocyte proliferation. Ihh has been implicated to be the downstream target of FGFR3 activation (21–23) and is well known to play a critical role in chondrocyte proliferation (24, 25). Based on these findings, we tested our speculation that Ihh may be the
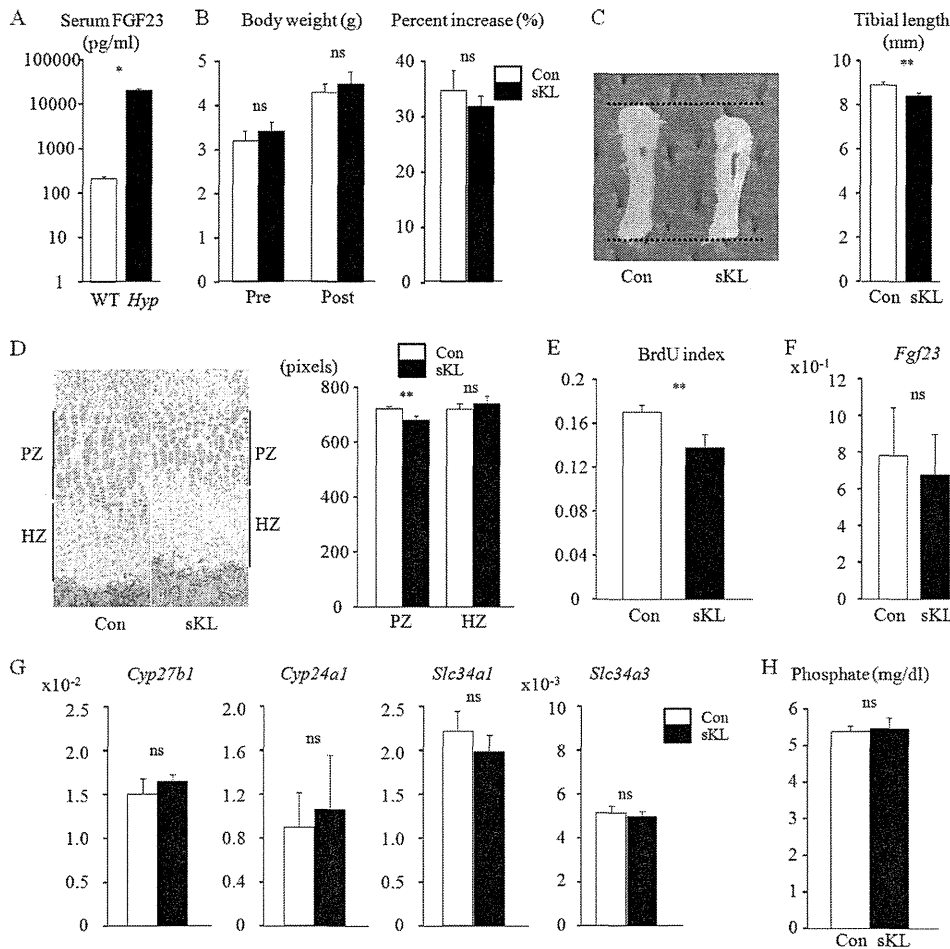
FIGURE 10. **Administration of sKL impairs chondrocyte proliferation in *Hyp* mice.** sKL (0.02 mg/kg) was intraperitoneally administered into *Hyp* mice for 3 days from postnatal day 7 and samples were collected on postnatal day 10. *A*, plasma FGF23 concentrations on postnatal day 10 in wild-type and *Hyp* mice (n = 3–4). *B*, body weights of *Hyp* mice on postnatal day 7 and day 10 and percent increases in body weight were calculated (n = 6–7). *C*, gross appearance of the tibia isolated on postnatal day 10 and tibial lengths were determined (n = 6–7). *D*, growth plates of tibiae were histologically analyzed by Hematoxylin and Eosin staining and the lengths of proliferating zones (*PZ*) and hypertrophic zones (*HZ*) were calculated (n = 6–7). *E*, BrdU staining was performed and the ratio of the number of BrdU-positive cells over total cells in the proliferating zone was determined (BrdU index) (n = 6–7). *F*, expression of *Fgf23* in the femur was determined by real-time RT-PCR (n = 3). *G*, expression levels of *Cyp27b1*, *Cyp24a1*, *Slc34a1*, and *Slc34a3* in the kidney were analyzed by real-time RT-PCR (n = 3–5). *H*, plasma levels of phosphate were measured (n = 6–7). The figures shown are the representative from at least three independent experiments. The values were expressed as mean ± S.E. *, $p < 0.001$; **, $p < 0.05$. *ns*, not significant.

downstream target of FGF23/sKL signaling and found that Ihh expression was reduced in the presence of FGF23/sKL and addition of Ihh protein partially reversed the impaired growth of metatarsals treated with FGF23/sKL. Since Ihh protein cannot fully rescue the growth impairment induced by FGF23/sKL signaling, other signals are likely involved in the action of FGF23/sKL on the suppression of chondrocyte proliferation. Because STAT1 has been shown to be activated in response to FGFR3 activation, which in turn results in the inhibition of chondrocyte proliferation (32), a signaling pathway through STAT1 activation may be involved in the FGF23/sKL-induced impairment in chondrocyte proliferation.

In XLH patients, it is well recognized that administration of phosphate and calcitriol is effective to improve linear growth, but is not sufficient to fully reverse impaired growth despite the correction in biochemical markers and rachitic changes (17, 33). This evidence may suggest the existence of factor(s) modulating the linear growth of XLH patients in addition to abnormal phosphate metabolism, and the current findings that FGF23 suppresses chondrocyte proliferation in the presence of

sKL may at least in part explain the reason why the correction in serum phosphate levels by administration of phosphate and calcitriol cannot fully regain impaired growth in XLH patients. If this mechanism is operative, the blockade of FGF23 signaling as a strategy for the treatment of XLH patients would be very promising because suppressing FGF23 signaling may have an additional benefit such as enhancing chondrocyte proliferation beyond its capacity to correct phosphate and vitamin D metabolism. Indeed, recent *in vivo* animal studies have provided evidence for the striking effectiveness of the blockade of FGF23 signaling pathways by the anti-FGF23 neutralizing antibody in the improvement of rickets and growth retardation in *Hyp* mice (34).

The significance of sKL in chondrocyte biology in humans remains largely unknown. Recent development in the ELISA system to detect human sKL has revealed that significant amounts of sKL are present in the human circulation (35); however, it is still controversial as to whether sKL in the circulation has any biological functions despite evidence demonstrating the biological function of sKL in animal models (12–14). Nev-

ertheless, the finding that sKL levels are greater in fetal life and childhood than that in adults may suggest that sKL may have more pronounced effects during these times (35–37). Since sKL levels in XLH patients have been shown to be comparable to those of control subjects (36), elevated FGF23 levels in these patients may have a significant impact on the signaling pathways exerted by FGF23/sKL. Our *in vivo* results using supraphysiologic concentrations of sKL may not be used to reach a definitive conclusion regarding the role of physiologic concentrations of sKL in the regulation of chondrocyte biology, but these findings may underline the significance of sKL, especially in fetal life and childhood when sKL levels are elevated and chondrocyte proliferation and maturation are actively operative.

In summary, we demonstrated that FGF23 possessed a non-canonical function where FGF23 suppressed chondrocyte proliferation and maturation in cooperation with sKL independent of phosphate metabolism, and this effect was partly mediated through FGFR3 and involved the suppression of Ihh expression. These lines of evidence add to our growing knowledge regarding signaling networks exerted by FGF23 and provide insights into the unrecognized function of FGF23 signaling that could be important for chondrocyte biology.

REFERENCES

1. Martin, A., David, V., and Quarles, L. D. (2012) Regulation and function of the FGF23/klotho endocrine pathways. *Physiol. Rev.* **92**, 131–155
2. Bai, X., Miao, D., Li, J., Goltzman, D., and Karaplis, A. C. (2004) Transgenic mice overexpressing human fibroblast growth factor 23 (R176Q) delineate a putative role for parathyroid hormone in renal phosphate wasting disorders. *Endocrinology* **145**, 5269–5279
3. Larsson, T., Marsell, R., Schipani, E., Ohlsson, C., Ljunggren, O., Tenenhouse, H. S., Jüppner, H., and Jonsson, K. B. (2004) Transgenic mice expressing fibroblast growth factor 23 under the control of the alpha1(I) collagen promoter exhibit growth retardation, osteomalacia, and disturbed phosphate homeostasis. *Endocrinology* **145**, 3087–3094
4. Shimada, T., Kakitani, M., Yamazaki, Y., Hasegawa, H., Takeuchi, Y., Fujita, T., Fukumoto, S., Tomizuka, K., and Yamashita, T. (2004) Targeted ablation of Fgf23 demonstrates an essential physiological role of FGF23 in phosphate and vitamin D metabolism. *J. Clin. Invest.* **113**, 561–568
5. Shimada, T., Urakawa, I., Yamazaki, Y., Hasegawa, H., Hino, R., Yoneya, T., Takeuchi, Y., Fujita, T., Fukumoto, S., and Yamashita, T. (2004) FGF-23 transgenic mice demonstrate hypophosphatemic rickets with reduced expression of sodium phosphate cotransporter type IIa. *Biochem. Biophys. Res. Commun.* **314**, 409–414
6. Yamashita, T., Yoshioka, M., and Itoh, N. (2000) Identification of a novel fibroblast growth factor, FGF-23, preferentially expressed in the ventrolateral thalamic nucleus of the brain. *Biochem. Biophys. Res. Commun.* **277**, 494–498
7. Quarles, L. D. (2012) Skeletal secretion of FGF-23 regulates phosphate and vitamin D metabolism. *Nat. Rev. Endocrinol.* **8**, 276–286
8. Urakawa, I., Yamazaki, Y., Shimada, T., Iijima, K., Hasegawa, H., Okawa, K., Fujita, T., Fukumoto, S., and Yamashita, T. (2006) Klotho converts canonical FGF receptor into a specific receptor for FGF23. *Nature* **444**, 770–774
9. Kurosu, H., Ogawa, Y., Miyoshi, M., Yamamoto, M., Nandi, A., Rosenblatt, K. P., Baum, M. G., Schiavi, S., Hu, M. C., Moe, O. W., and Kuro-o, M. (2006) Regulation of fibroblast growth factor-23 signaling by klotho. *J. Biol. Chem.* **281**, 6120–6123
10. Sitara, D., Kim, S., Razzaque, M. S., Bergwitz, C., Taguchi, T., Schüler, C., Erben, R. G., and Lanske, B. (2008) Genetic evidence of serum phosphate-independent functions of FGF-23 on bone. *PLoS Genet.* **4**, e1000154
11. Wang, H., Yoshiko, Y., Yamamoto, R., Minamizaki, T., Kozai, K., Tanne, K., Aubin, J. E., and Maeda, N. (2008) Overexpression of fibroblast growth factor 23 suppresses osteoblast differentiation and matrix mineralization in vitro. *J. Bone Miner. Res.* **23**, 939–948
12. Kurosu, H., Yamamoto, M., Clark, J. D., Pastor, J. V., Nandi, A., Gurnani, P., McGuinness, O. P., Chikuda, H., Yamaguchi, M., Kawaguchi, H., Shimomura, I., Takayama, Y., Herz, J., Kahn, C. R., Rosenblatt, K. P., and Kuro-o, M. (2005) Suppression of aging in mice by the hormone Klotho. *Science* **309**, 1829–1833
13. Liu, H., Fergusson, M. M., Castilho, R. M., Liu, J., Cao, L., Chen, J., Malide, D., Rovira, II, Schimel, D., Kuo, C. J., Gutkind, J. S., Hwang, P. M., and Finkel, T. (2007) Augmented Wnt signaling in a mammalian model of accelerated aging. *Science* **317**, 803–806
14. Doi, S., Zou, Y., Togao, O., Pastor, J. V., John, G. B., Wang, L., Shiizaki, K., Gotschall, R., Schiavi, S., Yorioka, N., Takahashi, M., Boothman, D. A., and Kuro-o, M. (2011) Klotho inhibits transforming growth factor-beta1 (TGF-β1) signaling and suppresses renal fibrosis and cancer metastasis in mice. *J. Biol. Chem.* **286**, 8655–8665
15. Shalhoub, V., Ward, S. C., Sun, B., Stevens, J., Renshaw, L., Hawkins, N., and Richards, W. G. (2011) Fibroblast growth factor 23 (FGF23) and α-klotho stimulate osteoblastic MC3T3.E1 cell proliferation and inhibit mineralization. *Calcif. Tissue Int.* **89**, 140–150
16. De Beur, S. M., Finnegan, R. B., Vassiliadis, J., Cook, B., Barberio, D., Estes, S., Manavalan, P., Petroziello, J., Madden, S. L., Cho, J. Y., Kumar, R., Levine, M. A., and Schiavi, S. C. (2002) Tumors associated with oncogenic osteomalacia express genes important in bone and mineral metabolism. *J. Bone Miner. Res.* **17**, 1102–1110
17. Friedman, N. E., Lobaugh, B., and Drezner, M. K. (1993) Effects of calcitriol and phosphorus therapy on the growth of patients with X-linked hypophosphatemia. *J. Clin. Endocrinol. Metab.* **76**, 839–844
18. Liu, S., Vierthaler, L., Tang, W., Zhou, J., and Quarles, L. D. (2008) FGFR3 and FGFR4 do not mediate renal effects of FGF23. *J. Am. Soc. Nephrol.* **19**, 2342–2350
19. Koshimizu, T., Kawai, M., Kondou, H., Tachikawa, K., Sakai, N., Ozono, K., and Michigami, T. (2012) Vinculin functions as regulator of chondrogenesis. *J. Biol. Chem.* **287**, 15760–15775
20. Kawai, M., Breggia, A. C., DeMambro, V. E., Shen, X., Canalis, E., Bouxsein, M. L., Beamer, W. G., Clemmons, D. R., and Rosen, C. J. (2011) The heparin-binding domain of IGFBP-2 has insulin-like growth factor binding-independent biologic activity in the growing skeleton. *J. Biol. Chem.* **286**, 14670–14680
21. Naski, M. C., Colvin, J. S., Coffin, J. D., and Ornitz, D. M. (1998) Repression of hedgehog signaling and BMP4 expression in growth plate cartilage by fibroblast growth factor receptor 3. *Development* **125**, 4977–4988
22. Li, C., Chen, L., Iwata, T., Kitagawa, M., Fu, X. Y., and Deng, C. X. (1999) A Lys644Glu substitution in fibroblast growth factor receptor 3 (FGFR3) causes dwarfism in mice by activation of STATs and ink4 cell cycle inhibitors. *Hum. Mol. Genet.* **8**, 35–44
23. Chen, L., Li, C., Qiao, W., Xu, X., and Deng, C. (2001) A Ser(365)→Cys mutation of fibroblast growth factor receptor 3 in mouse downregulates Ihh/PTHrP signals and causes severe achondroplasia. *Hum. Mol. Genet.* **10**, 457–465
24. Vortkamp, A., Lee, K., Lanske, B., Segre, G. V., Kronenberg, H. M., and Tabin, C. J. (1996) Regulation of rate of cartilage differentiation by Indian hedgehog and PTH-related protein. *Science* **273**, 613–622
25. Kobayashi, T., Soegiarto, D. W., Yang, Y., Lanske, B., Schipani, E., McMahon, A. P., and Kronenberg, H. M. (2005) Indian hedgehog stimulates periarticular chondrocyte differentiation to regulate growth plate length independently of PTHrP. *J. Clin. Invest.* **115**, 1734–1742
26. Faul, C., Amaral, A. P., Oskouei, B., Hu, M. C., Sloan, A., Isakova, T.,

Gutiérrez, O. M., Aguillon-Prada, R., Lincoln, J., Hare, J. M., Mundel, P., Morales, A., Scialla, J., Fischer, M., Soliman, E. Z., Chen, J., Go, A. S., Rosas, S. E., Nessel, L., Townsend, R. R., Feldman, H. I., St John Sutton, M., Ojo, A., Gadegbeku, C., Di Marco, G. S., Reuter, S., Kentrup, D., Tiemann, K., Brand, M., Hill, J. A., Moe, O. W., Kuro-O, M., Kusek, J. W., Keane, M. G., and Wolf, M. (2011) FGF23 induces left ventricular hypertrophy. *J. Clin. Invest.* **121,** 4393–4408

27. Imura, A., Iwano, A., Tohyama, O., Tsuji, Y., Nozaki, K., Hashimoto, N., Fujimori, T., and Nabeshima, Y. (2004) Secreted Klotho protein in sera and CSF: implication for post-translational cleavage in release of Klotho protein from cell membrane. *FEBS Lett.* **565,** 143–147

28. Chen, L., Adar, R., Yang, X., Monsonego, E. O., Li, C., Hauschka, P. V., Yayon, A., and Deng, C. X. (1999) Gly369Cys mutation in mouse FGFR3 causes achondroplasia by affecting both chondrogenesis and osteogenesis. *J. Clin. Invest.* **104,** 1517–1525

29. Wang, Y., Spatz, M. K., Kannan, K., Hayk, H., Avivi, A., Gorivodsky, M., Pines, M., Yayon, A., Lonai, P., and Givol, D. (1999) A mouse model for achondroplasia produced by targeting fibroblast growth factor receptor 3. *Proc. Natl. Acad. Sci. U.S.A.* **96,** 4455–4460

30. Segev, O., Chumakov, I., Nevo, Z., Givol, D., Madar-Shapiro, L., Sheinin, Y., Weinreb, M., and Yayon, A. (2000) Restrained chondrocyte proliferation and maturation with abnormal growth plate vascularization and ossification in human FGFR-3(G380R) transgenic mice. *Hum. Mol. Genet.* **9,** 249–258

31. Ornitz, D. M., and Marie, P. J. (2002) FGF signaling pathways in endochondral and intramembranous bone development and human genetic disease. *Genes Dev.* **16,** 1446–1465

32. Sahni, M., Ambrosetti, D. C., Mansukhani, A., Gertner, R., Levy, D., and Basilico, C. (1999) FGF signaling inhibits chondrocyte proliferation and regulates bone development through the STAT-1 pathway. *Genes Dev.* **13,** 1361–1366

33. Chesney, R. W., Mazess, R. B., Rose, P., Hamstra, A. J., DeLuca, H. F., and Breed, A. L. (1983) Long-term influence of calcitriol (1,25-dihydroxyvitamin D) and supplemental phosphate in X-linked hypophosphatemic rickets. *Pediatrics* **71,** 559–567

34. Aono, Y., Yamazaki, Y., Yasutake, J., Kawata, T., Hasegawa, H., Urakawa, I., Fujita, T., Wada, M., Yamashita, T., Fukumoto, S., and Shimada, T. (2009) Therapeutic effects of anti-FGF23 antibodies in hypophosphatemic rickets/osteomalacia. *J. Bone Miner. Res.* **24,** 1879–1888

35. Yamazaki, Y., Imura, A., Urakawa, I., Shimada, T., Murakami, J., Aono, Y., Hasegawa, H., Yamashita, T., Nakatani, K., Saito, Y., Okamoto, N., Kurumatani, N., Namba, N., Kitaoka, T., Ozono, K., Sakai, T., Hataya, H., Ichikawa, S., Imel, E. A., Econs, M. J., and Nabeshima, Y. (2010) Establishment of sandwich ELISA for soluble α-Klotho measurement: Age-dependent change of soluble α-Klotho levels in healthy subjects. *Biochem. Biophys. Res. Commun.* **398,** 513–518

36. Carpenter, T. O., Insogna, K. L., Zhang, J. H., Ellis, B., Nieman, S., Simpson, C., Olear, E., and Gundberg, C. M. (2010) Circulating levels of soluble klotho and FGF23 in X-linked hypophosphatemia: circadian variance, effects of treatment, and relationship to parathyroid status. *J. Clin. Endocrinol. Metab.* **95,** E352–357

37. Ohata, Y., Arahori, H., Namba, N., Kitaoka, T., Hirai, H., Wada, K., Nakayama, M., Michigami, T., Imura, A., Nabeshima, Y., Yamazaki, Y., and Ozono, K. (2011) Circulating levels of soluble alpha-Klotho are markedly elevated in human umbilical cord blood. *J. Clin. Endocrinol. Metab.* **96,** E943–947

A lightweight mainstream capnometer with very low dead space volume is useful monitor for neonates with spontanous and mechanical ventilation: Pilot study[*]

Daijiro Takahashi[1,2], Miyu Matsui[1], Takehiko Hiroma[1], Tomohiko Nakamura[1]

[1]Division of Neonatology, Nagano Children's Hospital, Nagano, Japan
[2]Department of Pediatrics, Fukuda Hospital, Kumamoto, Japan
Email: tnakamura@naganoch.gr.jp

ABSTRACT

Objects: The purpose of this study was to observe a correlation between $P_{ET}CO_2$ and $PaCO_2$ in intubated neonates under intermittent mandatory ventilation with spontaneous breathing. **Material and methods:** A total of 55 paired $P_{ET}CO_2$ measured by mainstream capnometry and $PaCO_2$ values were obtained from 4 intubated neonates in our neonatal intensive care units at Nagano Children's Hospital, Nagano, Japan. **Results:** $P_{ET}CO_2$ and $PaCO_2$ were significantly correlated ($r^2 = 0.928$, $p < 0.0001$). For samples in ventilated neonates with spontaneous breathing, maximum $P_{ET}CO_2$ and mean $P_{ET}CO_2$ correlated strongly with $PaCO_2$ (maximum $P_{ET}CO_2$: $r^2 = 0.9401$, $p < 0.0001$; mean $P_{ET}CO_2$: $r^2 = 0.8587$, $p < 0.0001$). Although $PaCO_2$ also correlated with minimum $P_{ET}CO_2$ ($r^2 = 0.2884$, $p < 0.01$) in ventilated infants with spontaneous breathing, a significant difference was seen with maximum $P_{ET}CO_2$ ($p < 0.05$) and mean $P_{ET}CO_2$ ($p < 0.05$) in the correlation coefficient r between $PaCO_2$ and $P_{ET}CO_2$. **Conclusion:** Present study showed that a good correlation exists between $P_{ET}CO_2$ and $PaCO_2$ in intubated neonates under intermittent mandatory ventilation with spontaneous breathing. Lightweight with low amounts of dead space mainstream capnometry can be used as noninvasive monitor in incubated neonates with spontaneous breathing.

Keywords: Capnography; Neonate

1. INTRODUCTION

Capnography, which displays the level and waveform of CO_2 in exhaled air, is a simple technique that appears to accurately indicate arterial PCO_2 ($PaCO_2$) and provides information on cell metabolism, blood perfusion, and alveolar ventilation [1-3]. The use of end-tidal CO_2 ($P_{ET}CO_2$) for monitoring and as a tool for verifying endotracheal tube (ETT) position is another common practice in the operating room and in adult and pediatric intensive care units [3]. This procedure was also introduced to neonatal intensive care units (NICUs), but there are limitations of the technique in smaller babies, especially for extremely low birth weight infants due to issues such as the weight of sensors or water droplets within circuits, dead space, and leakage from tracheal intubation tubes. Recently, a lightweight mainstream capnometer was developed. We have previously reported a strong correlation between $P_{ET}CO_2$ and $PaCO_2$ under controlled ventilation when tidal volume/body weight (TV/BW) was 6 - 15 mL/kg and the leakage rate was <60% in rabbits. Furthermore, under conditions of 6 mL/kg of tidal volume (TV), $PaCO_2$ was significantly increased by a dead space increase of only 1 mL, representing >7% of TV [4].

Capnometry is expected as one of the non-invasive monitor in NICUs. Although several investigators have demonstrated good relationships between values for $P_{ET}CO_2$ and $PaCO_2$ in infants [5-8], the value of capnometry in estimating $PaCO_2$ has been questioned during anesthesia with spontaneous ventilation [9,10]. On the other hand, while TV is larger than spontaneous breaths, $P_{ET}CO_2$ is close to the $PaCO_2$ and to that observed with voluntary maximal expiration [11]. The purpose of this study was to observe a correlation between $P_{ET}CO_2$ and $PaCO_2$ in intubated neonates under intermittent mandatory ventilation (IMV) with spontaneous breathing.

2. MATERIAL AND METHODS

A total of 55 paired $P_{ET}CO_2$ and $PaCO_2$ values were obtained from the 4 neonates who had been admitted to the NICU at Nagano Children's Hospital between April and July 2009. Neonates deemed as non-viable by the attending physician were excluded, as were those with

---

conditions such as acute shock, infection, or hemodynamic instability. Before enrollment into this study, informed consent was obtained from the parents or guardian of each infant. Study subjects comprised 4 neonates. Mean (±standard deviation (SD)) gestational age and birth weight were 36.7 ± 2.1 weeks and 2446 ± 487 g, respectively. Data on demographics, clinical characteristics, and laboratory findings for subjects were collected by referring to the clinical laboratory records.

The infants were ventilated mechanically using a time-cycled pressure-limited ventilator (Calliope®; Metran, Saitama, Japan). Peak inspiratory pressure (PIP), fraction of inhaled oxygen (FiO$_2$), inspiratory time, positive end expiratory pressure (PEEP) and respiratory rate were settled to provide the optimal arterial PaO$_2$ and PaCO$_2$ as defined by the neonatologists and were not manipulated for the purposes of the study.

Mainstream P$_{ET}$CO$_2$ was measured via a capnograph connected to the proximal end of the endotracheal tube (Cap-One®; TG-970P, Nihon-Kohden, Tokyo, Japan). Data was continuously recorded on a laptop computer using the software programmed by LabVIEW (National Instruments, Texas, USA) through CO$_2$ monitor (OLG-2800; Nihon-Kohden, Tokyo, Japan) each patients. We distinguished between spontaneous breaths and ventilator breaths on the basis of capnography for 20 s at the time of blood gas analysis. For each 20-s sample period, we determined the maximum, mean and minimum values of P$_{ET}$CO$_2$ (**Figure 1**). Measurements of P$_{ET}$CO$_2$ that did not show an alveolar plateau due to a large amount of leakage were excluded.

The tidal volume was measured by mainstream capnography (CO2SMO 8100, Fukuda Denshi, Tokyo, Japan). The leakage ratio was calculated using the following equation:

$$\text{Leakage ratio} = \frac{(\text{Inspiratory TV} - \text{Expiratory TV})}{\text{Inspiratory TV}} \times 100$$

Blood samples were drawn from indwelling arterial lines into a 0.1-mL heparinized syringe to prevent coagulation. Blood sampling was performed by heel puncture when arterial line was not placed. Measurements

were then immediately made using a bedside blood gas analyzer (ABL 700; Radiometer, Copenhagen, Denmark) for PaCO$_2$. Blood gas analysis was performed for the purposes of evaluation of the patient (including PaO$_2$, PaCO$_2$, electrolytes or lactate, etc.) only. Calibrations were performed automatically for the blood gas analyzer and the accuracy of the capnography was checked by 5% CO$_2$ gas cylinder.

All statistical analyses were conducted using SPSS Statistics version 17.0 (SPSS, Chicago, Illinois). To determine whether P$_{ET}$CO$_2$ were representative of PaCO$_2$, the relationship between P$_{ET}$CO$_2$ and PaCO$_2$ was analyzed by simple linear regression. The standard technique of Fisher's Z transformation was performed to determine whether a significant difference existed in the correlation coefficient r between PaCO$_2$ and each group of P$_{ET}$CO$_2$.

Furthermore, Bland-Altman plots were performed to assess measurements of P$_{ET}$CO$_2$. Bland-Altman plots demonstrate "good agreement" not only when differences between methods are consistent across all measurements but also when the differences are small. In a situation in which the difference between measurements is expected to change based on a third variable, Bland-Altman plots lose importance. Precision of P$_{ET}$CO$_2$ and the agreement between P$_{ET}$CO$_2$ and PaCO$_2$ were assessed by bias, SD and calculating the 95% confidence interval (CI) for the bias (bias = P$_{ET}$CO$_2$ – PaCO$_2$). Values of p < 0.05 were determined to be significant.

This study was carried out under the control of the Ethics Committee of Medicine and Medical Care, Nagano Children's Hospital, Nagano, Japan.

3. RESULTS

Mean TV/BW and leakage ratio were 7.3 ± 1.7 mL/kg and 9.5% ± 12.0%, respectively (**Table 1**). All patients were treated using sedative drugs.

P$_{ET}$CO$_2$ and PaCO$_2$ were significantly correlated (r^2 = 0.928, p < 0.0001). In the Bland-Altman plot test, the mean difference (bias) and SD of the differences for
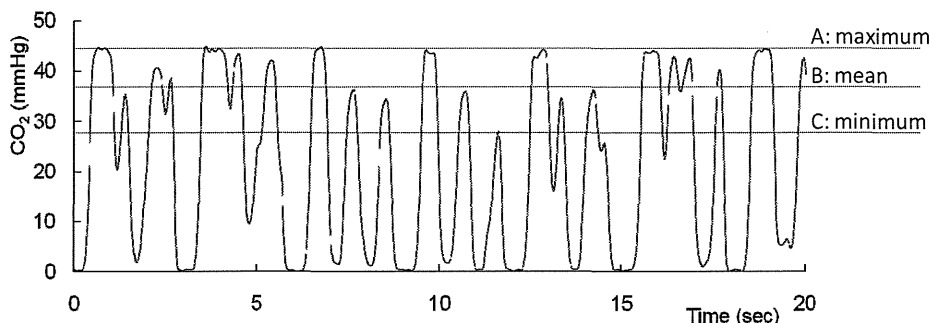

Figure 1. Continuous recording of P$_{ET}$CO$_2$. For each 20-s sample period, we determined maximum A, mean B and minimum C P$_{ET}$CO$_2$.

Table 1. Baseline characteristics.

Characteristics	Number of patients
Sex	
Male	3
Female	1
Inborn/Outborn	
Inborn	3
Outborn	1
Underlying disease	
Congenital heart disease	2
Intraventricular hemorrhage	1
Perioperative management	1
Gestational age (week)	
Mean ± SD	36.7 ± 2.1
Range	34 – 39
Birthweight (g)	
Mean ± SD	2446 ± 487
Range	1778 - 2894
Tidal volume/Body weight (mL/kg)	
Mean ± SD	7.3 ± 1.7
Range	4.8 - 8.6
Leakage ratio (%)	
Mean ± SD	9.5 ± 12.0
Range	0 - 27

$P_{ET}CO_2$ was −0.88 ± 2.69 mmHg (95% CI for the bias, −1.61 to −0.16 mmHg) (**Figure 2**). We chose the maximum for $P_{ET}CO_2$ on the basis of capnograms for each 20-s period at the time of blood gas analysis.

Due to breath-to-breath variation, we evaluated three measurements of $P_{ET}CO_2$ to determine which one most consistently and accurately predicted $PaCO_2$. From 55
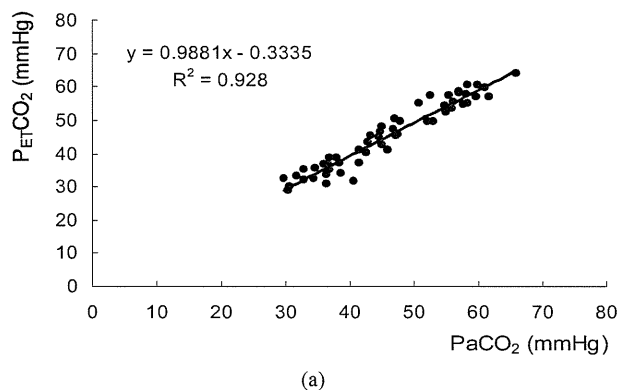
measurements, we have selected 24 paired $P_{ET}CO_2$ and $PaCO_2$ values which were obtained at the time when spontaneous breathing was present.

For samples in ventilated infants with spontaneous breathing, maximum $P_{ET}CO_2$ and mean $P_{ET}CO_2$ correlated strongly with $PaCO_2$ (maximum $P_{ET}CO_2$: $r^2 = 0.9401$, $p < 0.0001$; mean $P_{ET}CO_2$: $r^2 = 0.8587$, $p < 0.0001$). Although $PaCO_2$ also correlated with minimum $P_{ET}CO_2$ ($r^2 = 0.2884$, $p < 0.01$) in ventilated infants with spontaneous breathing, a significant difference was seen with maximum $P_{ET}CO_2$ ($p < 0.05$) and mean $P_{ET}CO_2$ ($p < 0.05$) in the correlation coefficient r between $PaCO_2$ and $P_{ET}CO_2$ (**Figures 3(a)-(c)**).

Bland-Altman analysis showed that $P_{ET}CO_2$ underestimated $PaCO_2$ by a mean difference (bias) of −0.175 ± 2.31 mmHg (95% CI for the bias, −1.15 to 0.799 mmHg) in the maximum $P_{ET}CO_2$, −5.01 ± 3.55 mmHg (95% CI for the bias, −6.50 to −3.51 mmHg) in mean $P_{ET}CO_2$, and −14.6 ± 8.82 mmHg (95%CI for the bias, −18.3 to −10.9 mmHg) in minimum $P_{ET}CO_2$ (**Figures 3(d)-(f)**).

4. DISCUSSION

Advances in the treatment of neonatal respiratory failure, including exogenous surfactant [12,13], inhaled nitric oxide (iNO) [14,15], and a growing repertoire of assisted ventilation strategies [16] have decreased morbidity and mortality rates. Patient monitoring has played a critical role in the safe and effective application of these advanced therapies.

Pulse oximetry provides a noninvasive method of assessing oxygenation and continuous surveillance of the partial pressure of arterial oxygen [17]. Maintaining $PaCO_2$ within the desired range by frequent arterial sampling can increase the need for multiple transfusions in the NICU [18], highlighting the need for methods of continuous non-invasive monitoring of CO_2 levels. Both hypocarbia and hypercarbia are detrimental to extremely low birth weight infants and have been implicated as
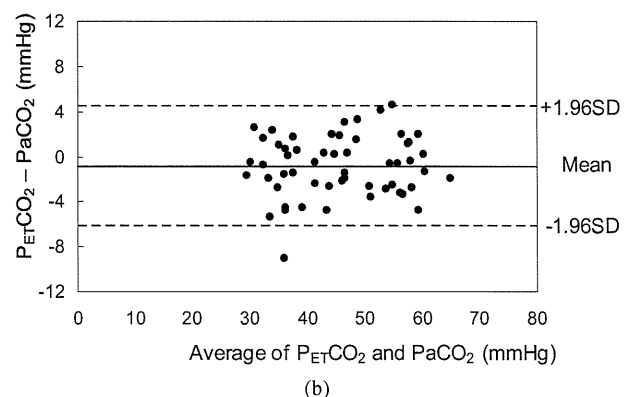

Figure 2. The relationship between $P_{ET}CO_2$ and $PaCO_2$ (a) and Bland-Altman plot shows bias against average values of $P_{ET}CO_2$ and $PaCO_2$ in ventilated infants (b). $P_{ET}CO_2$ and $PaCO_2$ were significantly correlated ($r^2 = 0.928$, $p < 0.0001$).
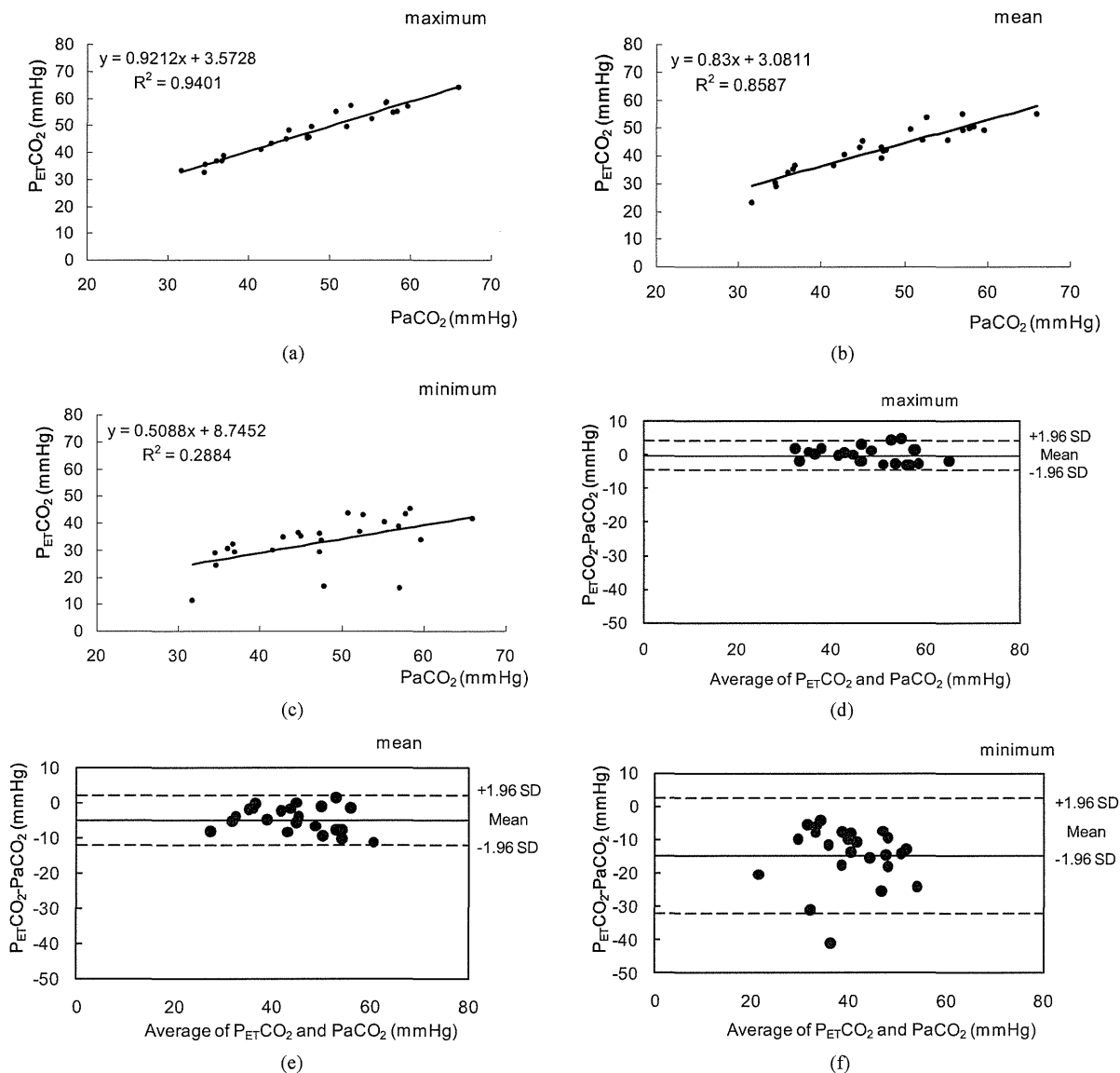
Figure 3. The relationship between $P_{ET}CO_2$ and $PaCO_2$ (a), (b) and (c) and Bland-Altman plot shows bias against average values of $P_{ET}CO_2$ and $PaCO_2$ in ventilated infants with spontaneous breathing (d), (e) and (f). Maximum $P_{ET}CO_2$ and mean $P_{ET}CO_2$ correlated strongly with $PaCO_2$. Conversely, $PaCO_2$ did not correlate with minimum $P_{ET}CO_2$.

causative factors in periventricular leukomalacia, intraventricular hemorrhage and chronic lung disease [19-21]. Critical event analyses have documented that hypoxemia secondary to depressed respiratory activity is a principal risk factor for near misses and death [22,23].

Monitoring of $P_{ET}CO_2$ is a simple and noninvasive technique that appears to accurately indicate $PaCO_2$ in a variety of clinical situations [1,24]. However, levels of $P_{ET}CO_2$ and $PaCO_2$ depend on ventilation, cardiac output, CO_2 output, and pulmonary function; a change in any of these will cause a change in $P_{ET}CO_2$ [25]. For instance, a growing degree of difference between $P_{ET}CO_2$ and $PaCO_2$ can indicate the severity of pulmonary embolism [26] or even the effects of thrombolytic therapy [27].

$P_{ET}CO_2$ varied appreciably from breath to breath. The reliability of this value under conditions of significant ventilation perfusion inequality or heterogeneous tidal volumes has thus been questioned [28]. In many cases, spontaneous breaths of variable tidal volumes far outnumbered ventilator breaths, but still contributed relatively little to alveolar minute ventilation. We found that maximum $P_{ET}CO_2$ during each sampling period showed the best correlation with $PaCO_2$. A number of investigators have suggested that larger tidal volumes are necessary to measure $P_{ET}CO_2$ accurately, as small (e.g., spontaneous) breaths may fail to "wash out" the anatomic dead space [11,29].

Weinger *et al.* [30] also found a wide range in differ-

ences between $P_{ET}CO_2$ and $PaCO_2$ over time. However, they measured mean peak $P_{ET}CO_2$ over a period of 8 min. Although averaging maximal $P_{ET}CO_2$ values over a longer time span might improve the stability and reliability of $PaCO_2$ - $P_{ET}CO_2$, assessing the respiratory status to measure $P_{ET}CO_2$ over a long time would be difficult. The respiratory apparatus might change second to second.

Takano *et al.* [31] reported that reliable $P_{ET}CO_2$ was obtained when a vital capacity maneuver was performed on each nonintubeted patient, indicating that full expiration to the maximal expiratory position is necessary for precise estimation of $PaCO_2$.

Comparison with spontaneous breathing, end tidal CO_2 measured from ventilated breath is close to the $PaCO_2$ and to that observed with a voluntary maximal expiration. This PCO_2 gradient between ventilator and spontaneous breathing indicates a large dead-space to tidal volume ratio; much of the expired CO_2 appearing with spontaneous breathing is diluted, with dead space air lowering the concentration at any point during expiration.

Although our prospective observational study revealed a good correlation and agreement between $PaCO_2$ and maximum $P_{ET}CO_2$, the present study included only a very small number of participants, and the conditions of patients were not constant. Furthermore, in children with congenital cyanotic heart disease, right-to-left intracardiac shunting reportedly causes an obligatory difference between $PaCO_2$ and $P_{ET}CO_2$ [32,33]. Our subjects included patients with congenital heart disease because they showed stable cardiorespiratory status in this study.

This study consisted of only a small number of participants, the statistical implications of repeated measurements in the same infants, and the conditions of the cases were not constant. In addition, we did not adjust for cardiac output their measurements, though differences in cardiac output are known to affect $P_{ET}CO_2$ measurements [25]. Therefore, we would like to study these issues in the future.

5. CONCLUSION

Our results indicate that a good correlation exists between $P_{ET}CO_2$ and $PaCO_2$ in intubated neonates under intermittent mandatory ventilation with spontaneous breathing. Furthermore, maximum $P_{ET}CO_2$ correlated strongly with $PaCO_2$ compared to minimum $P_{ET}CO_2$. Lightweight with low amounts of dead space mainstream capnometry can be used as noninvasive monitor in incubated neonates with spontaneous breathing.

6. ACKNOWLEDGEMENTS

REFERENCES

[1] Burton, G.W. (1966) The value of carbon dioxide monitoring during anaesthesia. *Anaesthesia*, **21**, 173-183. doi:10.1111/j.1365-2044.1966.tb02596.x

[2] Burton, G.W. (1969) Measurement of inspired and expired oxygen and carbon dioxide. *British Journal of Anaesthesia*, **41**, 723-730. doi:10.1093/bja/41.9.723

[3] Bhende, M.S. (2001) End-tidal carbon dioxide monitoring in pediatrics—Clinical applications. *Journal of Postgraduate Medicine*, **47**, 215-218.

[4] Takahashi, D., Hiroma, T. and Nakamura, T. (2011) $P_{ET}CO_2$ measured by a new lightweight mainstream capnometer with very low dead space volume offers accurate and reliable noninvasive estimation of $PaCO_2$. *Research and Reports in Neonatology*, **1**, 61-66.

[5] Meyer, R.E. and Short, C.E. (1985) Arterial to end-tidal CO_2 tension and alveolar dead space in halothane- or isoflurane-anesthetized ponies. *American Journal of Veterinary Research*, **46**, 597-599.

[6] Geiser, D.R. and Rohrbach, B.W. (1992) Use of end-tidal CO_2 tension to predict arterial CO_2 values in isoflurane-anesthetized equine neonates. *American Journal of Veterinary Research*, **53**, 1617-1621.

[7] Riker, J.B. and Haberman, B. (1976) Expired gas monitoring by mass spectrometry in a respiratory intensive care unit. *Critical Care Medicine*, **4**, 223-229. doi:10.1097/00003246-197609000-00002

[8] McEvedy, B.A., McLeod, M.E., Kirpalani, H., Volgyesi, G.A. and Lerman, J. (1990) End-tidal carbon dioxide measurements in critically ill neonates: A comparison of side-stream and mainstream capnometers. *Canadian Journal of Anesthesia*, **37**, 322-326. doi:10.1007/BF03005583

[9] Hagerty, J.J., Kleinman, M.E., Zurakowski, D., Lyons, A.C. and Krauss, B. (2002) Accuracy of a new low-flow sidestream capnography technology in newborns: A pilot study. *Journal of Perinatology*, **22**, 219-225. doi:10.1038/sj.jp.7210672

[10] Bhat, Y.R. and Abhishek, N. (2008) Mainstream end-tidal carbon dioxide monitoring in ventilated neonates. *Singapore Medical Journal*, **49**, 199-203.

[11] Kugelman, A., Zeiger-Aginsky, D., Bader, D., Shoris, I. and Riskin, A. (2008) A novel method of distal end-tidal CO_2 capnography in intubated infants: comparison with arterial CO_2 and with proximal mainstream end-tidal CO_2. *Pediatrics*, **122**, e1219-e1224. doi:10.1542/peds.2008-1300

[12] Lee, K., Khoshnood, B., Wall, S.N., Chang, Y., Hsieh, H.L. and Singh, J.K. (1999) Trend in mortality from respiratory distress syndrome in the United States, 1970-1995. *Journal of Pediatrics*, **134**, 434-440. doi:10.1016/S0022-3476(99)70200-3

[13] Rodriguez, R.J. and Martin, R.J. (1999) Exogenous surfactant therapy in newborns. *Respiratory Care Clinics of*

North America, **5**, 595-616.

[14] Wessel, D.L., Adatia, I., Van Marter, L.J., Thompson, J.E., Kane, J.W., Stark, A.R., *et al.* (1997) Improved oxygenation in a randomized trial of inhaled nitric oxide for persistent pulmonary hypertension of the newborn. *Pediatrics*, **100**, E7. doi:10.1542/peds.100.5.e7

[15] Cornfield, D.N., Maynard, R.C., de Regnier, R.A., Guiang, S.F., Barbato, J.E. and Milla, C.E. (1999) Randomized, controlled trial of low-dose inhaled nitric oxide in the treatment of term and near-term infants with respiratory failure and pulmonary hypertension. *Pediatrics*, **104**, 1089-1094. doi:10.1542/peds.104.5.1089

[16] Plavka, R., Kopecky, P., Sebron, V., Svihovec, P., Zlatohlavkova, B. and Janus, V. (1999) A prospective randomized comparison of conventional mechanical ventilation and very early high frequency oscillatory ventilation in extremely premature newborns with respiratory distress syndrome. *Intensive Care Medicine*, **25**, 68-75. doi:10.1007/s001340050789

[17] Dziedzic, K. and Vidyasagar, D. (1989) Pulse oximetry in neonatal intensive care. *Clinics in Perinatology*, **16**, 177-197.

[18] Madsen, L.P., Rasmussen, M.K., Bjerregaard, L.L., Nohr, S.B. and Ebbesen, F. (2000) Impact of blood sampling in very preterm infants. *Scandinavian Journal of Clinical and Laboratory Investigation*, **60**, 125-132. doi:10.1080/00365510050184949

[19] Giannakopoulou, C., Korakaki, E., Manoura, A., Bikouvarakis, S., Papageorgiou, M., Gourgiotis, D., *et al.* (2004) Significance of hypocarbia in the development of periventricular leukomalacia in preterm infants. *Pediatrics International*, **46**, 268-273. doi:10.1111/j.1442-200x.2004.01886.x

[20] Erickson, S.J., Grauaug, A., Gurrin, L. and Swaminathan, M. (2002) Hypocarbia in the ventilated preterm infant and its effect on intraventricular haemorrhage and bronchopulmonary dysplasia. *Journal of Paediatrics and Child Health*, **38**, 560-562. doi:10.1046/j.1440-1754.2002.00041.x

[21] Wallin, L.A., Rosenfeld, C.R., Laptook, A.R., Maravilla, A.M., Strand, C., Campbell, N., *et al.* (1990) Neonatal intracranial hemorrhage: II. Risk factor analysis in an inborn population. *Early Human Development*. **23**, 129-137. doi:10.1016/0378-3782(90)90136-7

[22] Strauss, R.G. (1991) Transfusion therapy in neonates. *American Journal of Disease of Children*, **145**, 904-911.

[23] Wiswell, T.E., Graziani, L.J., Kornhauser, M.S., Stanley, C., Merton, D.A., McKee, L., *et al.* (1996) Effects of hypocarbia on the development of cystic periventricular leukomalacia in premature infants treated with high-frequency jet ventilation. *Pediatrics*, **98**, 918-924.

[24] Gothard, J.W., Busst, C.M., Branthwaite, M.A., Davies, N.J. and Denison, D.M. (1980) Applications of respiratory mass spectrometry to intensive care. *Anaesthesia*, **35**, 890-895.
doi:10.1111/j.1365-2044.1980.tb03950.x

[25] Ornato, J.P., Garnett, A.R. and Glauser, F.L. (1990) Relationship between cardiac output and the end-tidal carbon dioxide tension. *Annals of Emergency Medicine*, **19**, 1104-1106. doi:10.1016/S0196-0644(05)81512-4

[26] Hatle, L. and Rokseth, R. (1974) The arterial to end-expiratory carbon dioxide tension gradient in acute pulmonary embolism and other cardiopulmonary diseases. *Chest*, **66**, 352-357. doi:10.1378/chest.66.4.352

[27] Verschuren, F., Heinonen, E., Clause, D., Roeseler, J., Thys, F., Meert, P., *et al.* (2004) Volumetric capnography as a bedside monitoring of thrombolysis in major pulmonary embolism. *Intensive Care Medicine*, **30**, 2129-2132. doi:10.1007/s00134-004-2444-9

[28] Capan, L.M., Ramanathan, S., Sinha, K. and Turndorf, H. (1985) Arterial to end-tidal CO_2 gradients during spontaneous breathing, intermittent positive-pressure ventilation and jet ventilation. *Critical Care Medicine*, **13**, 810-813. doi:10.1097/00003246-198510000-00007

[29] Evans, J.M., Hogg, M.I. and Rosen, M. (1977) Correlation of alveolar PCO_2 estimated by infra-red analysis and arterial PCO_2 in the human neonate and the rabbit. *British Journal of Anaesthesia*, **49**, 761-764. doi:10.1093/bja/49.8.761

[30] Weinger, M.B. and Brimm, J.E. (1987) End-tidal carbon dioxide as a measure of arterial carbon dioxide during intermittent mandatory ventilation. *Journal of Clinical Monitoring*, **3**, 73-79. doi:10.1007/BF00858353

[31] Takano, Y., Sakamoto, O., Kiyofuji, C. and Ito, K. (2003) A comparison of the end-tidal CO_2 measured by portable capnometer and the arterial PCO_2 in spontaneously breathing patients. *Respiratory Medicine*, **97**, 476-481. doi:10.1053/rmed.2002.1468

[32] Fletcher, R. (1991) The relationship between the arterial to end-tidal PCO_2 difference and hemoglobin saturation in patients with congenital heart disease. *Anesthesiology*, **75**, 210-221. doi:10.1097/00000542-199108000-00007

[33] Short, J.A., Paris, S.T., Booker, P.D. and Fletcher, R. (2001) Arterial to end-tidal carbon dioxide tension difference in children with congenital heart disease. *British Journal of Anaesthesia*, **86**, 349-353. doi:10.1093/bja/86.3.349

PEDIATRICS®

Qualitative Brain MRI at Term and Cognitive Outcomes at 9 Years After Very Preterm Birth

Sachiko Iwata, Tomohiko Nakamura, Eriko Hizume, Hideki Kihara, Sachio Takashima, Toyojiro Matsuishi and Osuke Iwata

The online version of this article, along with updated information and services, is located on the World Wide Web at:
http://pediatrics.aappublications.org/content/early/2012/04/17/peds.2011-1735

American Academy of Pediatrics
DEDICATED TO THE HEALTH OF ALL CHILDREN™

Qualitative Brain MRI at Term and Cognitive Outcomes at 9 Years After Very Preterm Birth

WHAT'S KNOWN ON THIS SUBJECT: Cross-sectional studies have demonstrated associations between the white matter injury and cognitive impairment in very preterm born children. Longitudinal studies confirmed the relationships between cerebral MRI at term and neurodevelopmental outcomes at up to 2 years old.

WHAT THIS STUDY ADDS: White matter injury (but not gray matter injury) on term MRI predicted cognitive impairments of very preterm born infants at 9 years old. Qualitative assessment of white matter signal intensities showed limited predictive values of cognitive impairments.

AUTHORS: Sachiko Iwata, MD,[a,b] Tomohiko Nakamura, MD, PhD,[b] Eriko Hizume, DOT,[c] Hideki Kihara, DPT, PhD,[c] Sachio Takashima, MD, PhD,[d] Toyojiro Matsuishi, MD, PhD,[a] and Osuke Iwata, MD[a,b]

[a]Centre for Developmental & Cognitive Neuroscience, Department of Paediatrics and Child Health, Kurume University School of Medicine, Kurume, Fukuoka, Japan; Divisions of [b]Neonatology, and [c]Rehabilitation, Nagano Children's Hospital, Nagano, Japan; and [d]Yanagawa Institute for Developmental Disabilities, International University of Health and Welfare, Fukuoka, Japan

abstract

OBJECTIVE: A prospective study was performed to assess the relationship between the appearance of cerebral MRI at term and the cognitive functioning at 9 years old in very preterm born infants.

METHODS: Seventy-six very preterm born infants (birth weight <1500 g or gestational age ≤32 weeks) obtained cerebral MRI at term-equivalent period, which was assessed by using established composite scores for the white and gray matter; cognitive outcomes at 9 years old were assessed in 60 subjects by using Wechsler Intelligence Scale for Children, Third Edition.

RESULTS: Mildly low scores on the different IQ indices (<85) were observed in 23.3% (verbal IQ), 41.7% (performance IQ), and 30.0% (full-scale IQ) of the cohort, whereas moderately low scores (<70) were noted in 3.3% (verbal IQ), 11.7% (performance IQ), and 11.7% (full-scale IQ); cerebral palsy was diagnosed in 10.0%, whereas special assistance at school was required in 56.7%. Abnormal white matter appearances predicted mildly low verbal, performance, and full-scale IQs; moderately low performance and full-scale IQs; cerebral palsy; and the requirement for special assistance at school. Abnormal white matter appearances predicted mild cognitive impairment even after the adjustment for known clinical risk factors. In contrast, abnormal gray matter appearances did not predict any of the outcome measures.

CONCLUSIONS: In a cohort of very preterm born infants, abnormal white matter appearance on term MRI showed consistent associations with cognitive impairments at 9 years old, further supporting the benefit of obtaining term MRI for very preterm born infants. *Pediatrics* 2012;129:e1138–e1147

The recent remarkable increase in the survival rate for very preterm born infants raised a concern on their long-term neurodevelopmental outcome.[1] The incidence of severe types of neurologic deficits, such as deafness, blindness, and cerebral palsy, have been declining in part because of the reduced incidence of severe cerebral injury, such as periventricular hemorrhagic infarction and periventricular leukomalacia (PVL).[2,3] In contrast, cognitive impairments are increasingly recognized as a prominent form of neurodevelopmental disorders in very preterm born infants.[4,5] The range of cognitive functioning of very preterm born infants at school age is various, yet significantly below that of term-born peers, with more than half of these children requiring special assistance at school.[6–9] To provide timely interventions, early prediction of neurodevelopmental impairments is essential.

Thus far, cerebral MRI has been used to identify structural brain abnormalities and related developmental impairments.[10] MRI studies of very preterm born children at school age demonstrated consistent associations between white matter volume reduction and cognitive impairments.[11–13] Recent studies have demonstrated the relationships between white matter abnormalities on term MRI and cognitive outcomes in very preterm born infants at 1 to 2 years old.[14–16] Additional studies with longer follow-up periods are still required, because neurodevelopmental assessments performed at early childhood period may not reflect cognitive functioning at school age and thereafter,[17–19] either because of the limited reliability of early assessment tools or because cognitive function itself may significantly alter under the influence of numerous intrinsic/extrinsic factors such as plasticity, compensation, reorganization of injured brain, environment, and education.

We conducted a prospective observational study in very preterm born infants hospitalized at a single tertiary center to test the hypothesis that abnormal MRI findings at term-equivalent age predict long-term cognitive impairments at 9 years old.

METHODS

Ethical approval was obtained from the ethics committee of Nagano Children's Hospital. Informed parental consent was obtained for each participating infant.

Study Population

The NICU of Nagano Children's Hospital is the only level III unit within the province of Nagano, which covers the population of ~2.5 million people including its neighbor provinces. Preterm infants with birth weight <1500 g and/or gestational age <34 weeks are enrolled into a domestic follow-up program for very preterm born infants at the time of discharge; we aim to obtain cerebral MRI between 38 and 42 weeks corrected age; neurodevelopmental outcomes are assessed at 18 and 36 months corrected age and 6 years chronological age by using individualized assessment tools.

Of 1156 newborn infants who were hospitalized between August 1995 and March 2001, 380 infants met the entry criteria of the follow-up program. However, 236 subjects were transferred to local level I/II units before discharge, and mothers of 27 subjects moved back to their home provinces after giving birth in Nagano (giving birth at parents' home site is common in Japan[20]); these infants were followed-up at their local hospitals (Fig 1). The remaining 117 subjects were enrolled into the follow-up program, whose cognitive outcome at 6 years old have been reported elsewhere.[21] For the current study, we recruited 76 very preterm born infants (birth weight <1500 g and/or gestational age ≤32

weeks) from the follow-up program, excluding 14 infants with major chromosomal abnormality or multiple congenital malformation, 2 infants with gestational age >32 weeks and birth weight ≥1500 g, and 25 infants whose MRI was not obtained before 42 weeks corrected age (Fig 1).

MRI Scans and Assessments

T1- and T2-weighted imaging and fluid-attenuated inversion recovery (FLAIR) imaging were obtained by using a 0.5-Tesla MRI system (Gyroscan NT5, Phillips, Best, Netherlands). The MRI methods used were T1-weighted imaging (repetition time, 384 milliseconds; echo time, 18 milliseconds), T2-weighted imaging (repetition time, 4000 milliseconds; echo time, 120 milliseconds), and FLAIR imaging (inversion time, 1800 milliseconds; repetition time, 6000 milliseconds; echo time, 140 milliseconds), with a slice thickness of 6 mm and an imaging matrix of 256 × 256 (Fig 2). Two investigators, blind to patient details, examined each scan independently; the evaluations of 1 investigator were used only for the assessment of interobserver variability[21]; all other results were based on the assessments of the other investigator.

We used an established scoring system for immature brain on T1- and T2-weighted imaging,[15,22] which consists of 5 and 3 subcategories for the white matter and gray matter, respectively. Each subcategory used a 3-point scale to give composite scores; abnormal findings in the white matter were then classified into no (score 5–6), mild (score 7–9), moderate (score 10–12), and severe (score 13–15) abnormality; no subject was ultimately assigned into severe abnormality in the current study population; abnormal findings in the gray matter were divided into 2 groups of normal (score 3–5) and abnormal (score 6–9). For the evaluation of the white matter, the presence of diffuse excessive high signal intensity (DEHSI)

```
┌─────────────────────────────────────────────┐
│ 1156 hospitalized between 08/1995 and 03/2001 │
│ - 380 <1500 g and/or <34 weeks' gestational age │
└─────────────────────────────────────────────┘
```
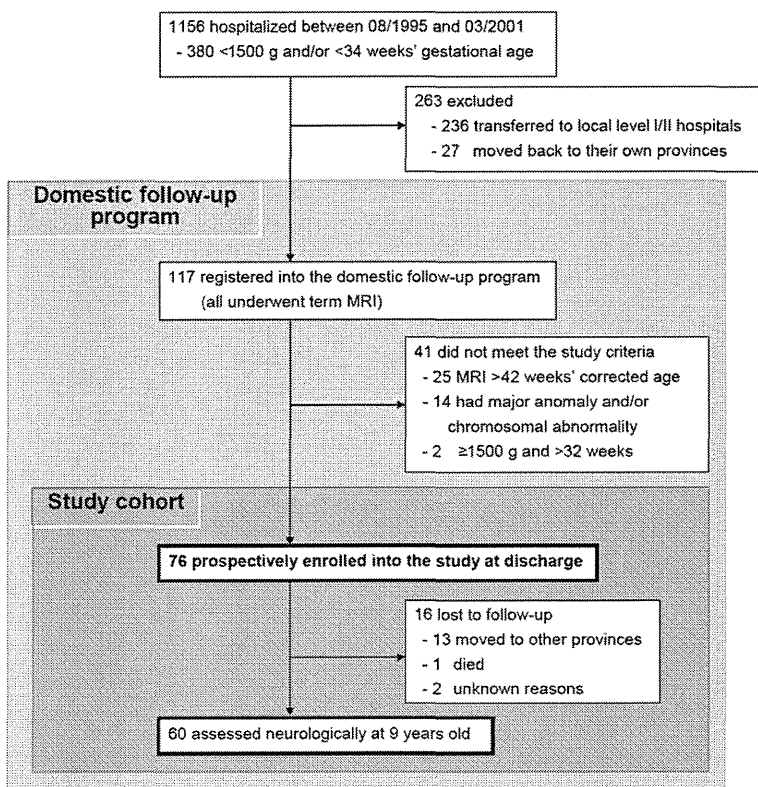
FIGURE 1

Flow of participants through the longitudinal study. During the study period, 380 infants met the criteria for the domestic follow-up program; however 263 subjects, who were either transferred to local hospitals before discharge or moved back to their parents' own provinces after discharge, were unavailable. Of 117 subjects who were enrolled to the follow-up program, 76 very preterm born infants without major congenital diseases were recruited for the prospective study.

on T2-weighted imaging and abnormal signal intensity on FLAIR imaging were also identified; FLAIR imaging was classified into 4 grades of normal, mildly abnormal (mild to moderate low-intensity), moderately abnormal (low-intensity equivalent to cerebrospinal fluid), and severely abnormal (widespread heterogeneous intensity; no subject was ultimately assigned into this grade; Fig 2 A and B).[21]

Outcome Measures

At 9 years old (chronological age), the Wechsler Intelligence Scale for Children, Third Edition was performed to assess verbal, performance, and full-scale IQs by an experienced psychologist who was blind to the MRI data. At the same time, the presence of hypertonicity, hyperreflexia, dystonia, and spasticity was assessed to identify cerebral palsy by consultant neonatologists; parents were also asked whether their children required special assistance at school because of problems in social, emotional, and behavioral adaptation.

Data Analysis

To assess the potential bias on the participants, background clinical variables were compared between the study cohort and their peers who were excluded because of the late timing of MRI scans by using analysis of variance, χ^2 test, or Fisher exact test, as appropriate. The relationship between MRI findings was assessed by using Spearman rank correlation coefficient. For the purpose of additional analyses, MRI findings were dichotomized into normal or abnormal (mild to severe). The outcome

measures were compared between subjects with or without abnormal MRI findings by using analysis of variance, χ^2 test, or Fisher exact test, as appropriate. The predictive ability of abnormal MRI findings on the outcome measures, including mild (IQ <85) and moderate (IQ <70) cognitive impairments, was assessed by using logistic regression analysis (verbal IQ <70 was not used as a dependent variable because of only 2 corresponding subjects).[23] For dependent variables with incidence >10 (IQs <85 and requirement for special assistance at school), the predictive ability of MRI findings were assessed with adjustment for known clinical risk factors of cognitive impairments, such as gestational age <28 weeks and cystic PVL; birth weight, which showed marked collinearity with gestational age, and severe intraventricular hemorrhage, which corresponded to only 1 subject at 9 years old, were not entered into the multivariate model. We aimed to use additional cofactors from the clinical variables listed in the Table 1 on the basis of the results from univariate analysis; eventually no variable was included because of the lack of correlations between adverse outcomes and clinical variables other than the gestational age and cystic PVL.

RESULTS

The 76 subjects within the study cohort had significantly greater birth weight, shorter duration on the positive pressure ventilation, and smaller incidence of intrauteral growth restriction compared with their 25 peers, whose MRI was acquired after 42 weeks' corrected age; no difference was observed for other background variables (Table 1).

MRI Findings at Term

Interrater reliabilities for the category assignments of the white matter and gray matter were $\kappa = 0.80$ and $\kappa = 0.82$
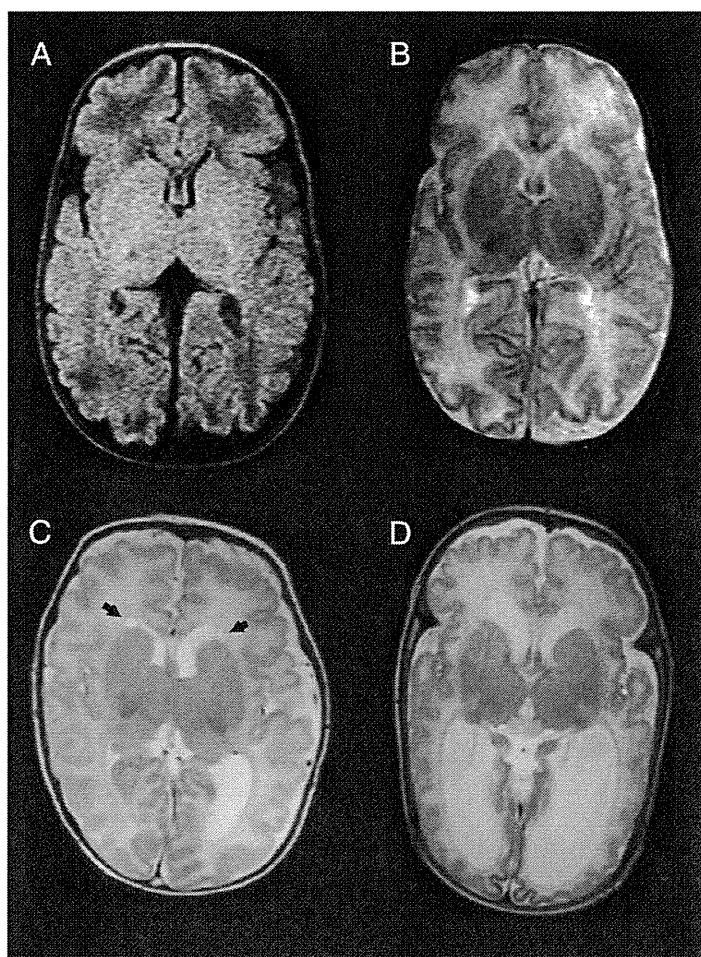
FIGURE 2
Representative MRI findings: A and B, Term MRI of an infant born at 28 weeks' gestation. The signal intensity of the white matter is excessively low on FLAIR imaging (A) and significantly increased on T2-weighted imaging (B). Except for mildly immature patterns of myelination of the posterior limb of the internal capsule and cortical folding, no abnormal cerebral architecture is noted. C, T2-weighted imaging of an infant born at 30 weeks' gestation demonstrates mild ventricular dilatation, bilateral periventricular cysts (arrows), and mild volume reduction of the gray and white matter. The architecture of the central gray and white matter is relatively preserved. D, T2-weighted imaging of an infant born at 25 weeks' gestation shows moderate dilatation of the lateral ventricles and moderate atrophy of the gray and white matter with an abnormal cortical folding pattern.

respectively. Agreement in the evaluation of DEHSI (T2-weighted imaging) and abnormal white matter signal intensity (FLAIR imaging) was also high (κ = 0.65 and κ = 0.78, respectively). Of 76 infants, abnormal high composite scores for the white matter and gray matter were observed in 24 (31.6%) and 16 (21.1%) infants, respectively, whereas DEHSI on T2-weighted imaging and abnormal white matter intensity on FLAIR imaging was noted in 13 (17.1%) and 58 (76.3%) infants, respectively. The presence of

white matter abnormalities based on composite scores was positively correlated with the presence of gray matter abnormalities (r = .60, P < .001), DEHSI on T2-weighted imaging (r =.34, P < .005), and abnormal white matter signal intensity on FLAIR imaging (r = .23, P < .05).

Neurodevelopmental Outcomes

At age 9 years, 16 subjects were lost to follow-up because of family relocation to other provinces (n = 13), mortality by an

accident (n = 1), or lost contact (n = 2; follow-up rate, 78.9%). Moderately low verbal, performance, and full-scale IQs <70 were recorded in 2, 7, and 7 subjects, respectively, whereas mildly low IQs <85 were noted in 14, 25, and 18 subjects, respectively. Cerebral palsy was diagnosed in 6 subjects; parents of 34 subjects reported the requirement for special assistance at school.

Term MRI Findings and Neurodevelopmental Outcomes

Subjects with abnormal white matter appearances based on the composite assessment had lower verbal (P< .005), performance (P < .001) and full-scale (P < .001) IQs, a higher incidence of cerebral palsy (P < .05), and a greater rate of subjects who require special assistance at school (P < .005) compared with their peers with normal findings (Table 2). Neither abnormal gray matter appearances nor DEHSI on T2-weighted imaging were associated with any of the outcome measures (Tables 3 and 4). Subjects with abnormal white matter intensities on FLAIR imaging had lower verbal and full-scale IQs (both P < .05) compared with their peers with normal findings (Table 5).

The presence of white matter injury defined by the composite assessment predicted mildly low verbal (odds ratio [OR] 6.3, 95% confidence interval [CI] 1.7–23.9), performance (OR 7.1, 95% CI 2.2–22.8), and full-scale (OR 8.3, 95% CI 2.4–29.1) IQs, moderately low performance (OR 12.7, 95% CI 1.4–114.0) and full-scale (OR 12.7, 95% CI 1.4–114.0) IQs, incidence of cerebral palsy (OR 10.0, 95% CI 1.1–92.1), and the requirement for special assistance at school (OR 7.0, 95% CI 2.0–24.6) (Tables 6 and 7; see online Supplemental Table 8 for the predictive value of each element from the composite assessment). After the effect was adjusted for gestational age and cystic PVL, significant

TABLE 1 Patients' Characteristics

	Study Cohort ($n = 76$)	Exclusion Due to Late MRI ($n = 25$)	P
Clinical variables			
Birth wt, g[a]	1118 ± 262 (560–1747)	884 ± 273 (483–1580)	<.001
Gestational age, wk[a]	28.6 ± 2.5 (23.7–34.6)	27.5 ± 2.1 (23.4–32.6)	
Female gender	30 (39)	13 (52)	
Multiple birth	22 (29)	11 (44)	
Intrauterine growth restriction <2 SD below the average for gestational age	8 (11)	10 (40)	<.005
Antenatal steroids	29 (38)	9 (36)	
Days on positive pressure ventilation[a]	39.2 ± 40.1 (0–274)	67.8 ± 39.6 (4–186)	<.001
Chronic lung disease with oxygen requirement on day 28- or 36-wk corrected age	26 (34)	14 (56)	
Symptomatic patent ductus arteriosus	23 (30)	8 (32)	
Necrotizing enterocolitis with requirement for surgical intervention	2 (3)	0 (0)	
Intraventricular hemorrhage, grade III/IV based on Papile classification	2 (3)	0 (0)	
Cystic periventricular leukomalacia	11 (14)	3 (12)	

Values are shown as the number of corresponding subjects (%). P values are from χ^2 test, Fisher exact test or analysis of variance.
[a] Mean ± SD (range).

TABLE 2 Neurodevelopmental Outcome at 9 Years in Subjects With or Without Abnormal MRI Findings: Composite Assessment of White Matter

	Normal ($n = 37$)	Abnormal ($n = 23$)	P
IQ			
Verbal	100.8 ± 12.9	88.7 ± 17.0	<.005
Performance	93.5 ± 12.4	78.6 ± 17.5	<.001
Full scale	97.0 ± 11.2	82.3 ± 16.6	<.001
Incidence of cerebral palsy (%)	1 (3)	5 (22)	<.05
Requirement for special assistance at school (%)	15 (41)	19 (83)	<.005

Values are shown as the number of corresponding subjects (%) or mean ± SD. P values are from χ^2 test Fisher exact test, or analysis of variance.

TABLE 3 Neurodevelopmental Outcome at 9 Years in Subjects With or Without Abnormal MRI Findings: Composite Assessment of Gray Matter

	Normal ($n = 46$)	DEHSI ($n = 14$)
IQ		
Verbal	96.4 ± 15.4	95.1 ± 17.0
Performance	88.3 ± 16.0	86.1 ± 17.3
Full scale	91.8 ± 15.0	90.1 ± 16.4
Incidence of cerebral palsy (%)	4 (9)	2 (14)
Requirement for special assistance at school (%)	26 (57)	8 (57)

Values are shown as the number of corresponding subjects (%) or mean ± SD.

predictive ability of abnormal white matter appearances was still identified on mildly low verbal (OR 6.2, 95% CI 1.5–25.1), performance (OR 6.0, 95% CI 1.7–20.9), and full-scale (OR 6.3, 95% CI 1.7–23.4) IQs, as well as the requirement for special assistance at school (OR 5.9,

95% CI 1.6–22.2; Table 6). The presence of abnormal gray matter appearance identified by the composite assessment and DEHSI on T2-weighted imaging did not predict any of the outcome measures. Abnormal white matter intensities on FLAIR imaging predicted verbal

IQ (OR 10.4, 95% CI 1.1–98.7) only after adjustment for gestational age and cystic PVL.

DISCUSSION

In a cohort of very preterm born infants, we have demonstrated consistent associations between abnormal white matter appearances on term MRI and cognitive impairments, incidence of cerebral palsy, and requirement for special assistance at school at 9 years old. In contrast, abnormal gray matter appearances did not predict cognitive outcomes. Our current findings supported the benefit of obtaining cerebral MRI at term after very preterm birth to identify a subset of infants who may require additional follow-up supports.

Abnormal White Matter Appearance and Cognitive Outcome

Composite Assessment of White Matter and Outcome

The impact of white matter injury in very preterm born children has thus far been emphasized in conjunction with later visual perceptual impairment; impaired ability to process and comprehend the visual input has been linked with lower performance IQ.[13,24–26] Our current findings suggest that the white matter injury in very preterm born infants may also be responsible for the impairment in language processing tasks. In addition to the associations with the incidence of cognitive impairment and cerebral palsy, abnormal white matter appearances were associated with the requirement for special assistance at school; this is not surprising given the relationship between a child's cognitive ability and adaptation to school after very preterm birth.[4,27] Early diagnosis of cognitive impairment is still challenging;[17–19] however, term MRI may help screen a group of very preterm born infants at increased risks of cognitive impairment. Future studies need to test

TABLE 4 Neurodevelopmental Outcome at 9 Years in Subjects With or Without Abnormal MRI Findings: Qualitative Assessment of White Matter Signal Intensities on T2-Weighted Imaging

	Normal (n = 50)	DEHSI (n = 10)
IQ		
Verbal	96.8 ± 16.2	92.5 ± 12.4
Performance	88.3 ± 15.6	85.2 ± 19.5
Full scale	92.1 ± 15.0	88.0 ± 16.4
Incidence of cerebral palsy (%)	5 (10)	1 (10)
Requirement for special assistance at school (%)	27 (54)	7 (70)

Values are shown as the number of corresponding subjects (%) or mean ± SD.

TABLE 5 Neurodevelopmental Outcome at 9 Years in Subjects With or Without Abnormal MRI Findings: Qualitative Assessment of White Matter Signal Intensities on FLAIR Imaging

	Normal (n = 16)	Abnormal (n = 44)	P
IQ			
Verbal	104.6 ± 16.2	93.1 ± 14.4	<.05
Performance	93.4 ± 12.2	85.7 ± 17.0	
Full scale	99.4 ± 13.2	88.5 ± 14.9	<.05
Incidence of cerebral palsy (%)	1 (6)	5 (11)	
Requirement for special assistance at school (%)	7 (44)	27 (61)	

Values are shown as the number of corresponding subjects (%) or mean ± SD. P values are from χ^2 test, Fisher exact test, or analysis of variance.

the hypothesis by using domain-specific assessment tools of cognitive functioning.

Pattern of White Matter Injury in the Study Cohort

Because the survival rate of very preterm born infants at Nagano Children's Hospital was reasonably fair (survival rates of infants born at 23–24 [68%] and 25–26 [79%] weeks' gestation between 1995 and 2001 were comparable to average rates for Japanese level III units in 2005[28]), background characteristics, such as low rates of antenatal steroid and inborn admission, may negatively influence the quality of survival. However, in our study population, extensive white matter injury was rare; even in the subjects with cystic PVL (our cohort had a relatively high incidence of cystic PVL), most lesions were small and focal and were rarely accompanied by marked white matter atrophy. The small incidence of severe intraventricular hemorrhage may contribute to white matter sparing; subjects with extensive white matter injury might be excluded from the cohort because of selection biases; however,

moderate to severe white matter injury was also rare for subjects who were excluded from the cohort because of the late timing of MRI scans. In addition to the clinical backgrounds, the threshold of the injury-score assignment in our institution might be higher compared with the original classification,[15] because interinstitutional variations of qualitative MRI assessments are common.[21,29,30] However, given the high interrater agreement of the MRI assessment, there would be only limited influence of bias on the current data interpretation.

Abnormal White Matter Signal Intensity and Outcome

In our previous study in a cohort of moderately preterm born infants, the presence of DEHSI on term T2-weighted imaging (observed in 17% of the subjects) was associated with low full-scale IQs, whereas abnormal white matter intensities on FLAIR imaging (63%) was association with unfavorable performance and full-scale IQs at 6 years old; abnormal findings on FLAIR imaging were mainly associated with mild cognitive impairments, whereas DEHSI

appeared to be specific to relatively more severe impairments.[21] In our current study, which prospectively followed up a part of the previous cohort with more strict entry criteria in gestational age and timing of MRI scans, associations with performance IQ were not observed for these abnormal signal intensities; instead, a modest correlation was observed between abnormal intensities on FLAIR (but not T2-weighted) imaging and verbal IQ. It is unclear why abnormal findings on term FLAIR imaging was associated with different IQ domains at different developmental stages. Standard cognitive batteries may be insensitive to subtle verbal impairments at earlier ages, and the difference might be caused by chance given the limited associations between abnormal signal intensities and cognitive outcomes. Regardless of the explanation, the evaluation of term MRI based solely on the white matter signal intensity may not provide precise estimation of long-term outcomes; the composite assessment should be prioritized to other MRI markers.

Abnormal Gray Matter Appearance and Outcome

In very preterm born children, reduced cortical gray matter volume has also been associated with poor cognitive outcome at school age.[11,31,32] In our current study, abnormal gray matter appearances at term were associated with the presence of white matter injury but not with any of the outcome measures at 9 years old. Previous studies observed a stronger correlation of cognitive outcomes with white matter injury compared with gray matter injury,[15,33] which is consistent with our current findings. Cortical gray matter lesions may contribute less to the later cognitive functioning; neurologic functioning associated with gray matter injury might be affected more by repairing process, plasticity, and extrinsic factors such as education and

TABLE 6 Predictive Ability of MRI Findings on Neurodevelopmental Outcomes at 9 Years

	n	Verbal IQ <85 (n = 14)		Performance IQ <85 (n = 25)		Full-scale IQ <85 (n = 18)		Performance IQ <70 (n = 7)		Full-scale IQ <70 (n = 7)		Cerebral Palsy (n = 6)		Special Assistance (n = 34)	
		OR	(95% CI)	OR	(95% CI)	OR	(95% CI)	OR	(95% CI)	OR	(95% CI)	OR	(95% CI)	OR	(95% CI)
Univariate analysis															
Clinical variables															
Birth wt <1000 g	19	0.5	(0.1–2.1)	1.9	(0.6–5.8)	1.1	(0.3–3.6)	0.9	(0.2–4.8)	0.3	(0.0–2.9)	1.1	(0.2–6.5)	0.8	(0.3–2.4)
Gestational age <28 wk	23	2.8	(0.8–9.4)	2.7	(0.9–7.9)	5.6	(1.7–18.7)**	4.9	(0.9–27.6)	2.4	(0.5–11.8)	1.7	(0.3–9.2)	2.4	(0.8–7.2)
Female gender	24	0.3	(0.1–1.3)	1.0	(0.4–2.9)	1.3	(0.4–4.0)	0.6	(0.1–3.2)		a	3.4	(0.6–20.3)	0.6	(0.2–1.8)
Multiple birth	18	2.1	(0.6–7.4)	0.4	(0.1–1.4)	0.9	(0.3–2.9)	0.9	(0.2–5.3)	1.9	(0.4–9.5)	0.4	(0.1–4.0)	0.7	(0.2–2.1)
Intrauterine growth restriction	6	0.6	(0.1–5.9)	1.5	(0.3–7.9)	1.2	(0.2–7.2)		a	1.6	(0.2–16.1)		a	0.7	(0.1–4.0)
Antenatal steroids	23	0.9	(0.3–3.0)	0.5	(0.2–1.4)	0.7	(0.2–2.3)		a	0.2	(0.0–2.1)		a	0.6	(0.2–1.6)
Chronic lung disease	21	1.6	(0.5–5.3)	0.8	(0.3–2.4)	1.8	(0.6-5.6)	0.3	(0.0–2.5)	0.7	(0.1–4.1)	0.3	(0.0–3.1)	1.0	(0.4–3.0)
Symptomatic patent ductus arteriosus	17	1.6	(0.4–5.6)	1.0	(0.3–3.0)	1.4	(0.4–4.7)	0.4	(0.0–3.5)	1.0	(0.2–5.8)	2.9	(0.5–15.8)	1.1	(0.4–3.5)
Necrotizing enterocolitis	1		a		a		a		a		a		a		a
Intraventricular hemorrhage (grade III or IV)	1		a		a		a		a		a		a		a
Cystic PVL	10	0.8	(0.2–4.3)	7.8	(1.5–40.7)*	2.8	(0.7–11.4)	4.9	(0.9–26.9)	2.3	(0.4–13.7)	2.9	(0.5–18.4)	9.0	(1.1–76.4)*
Abnormal MRI findings															
Composite assessment															
White matter	23	6.3	(1.7–23.9)**	7.1	(2.2–22.8)***	8.3	(2.4–29.1)***	12.7	(1.4–114.0)*	12.7	(1.4–114.0)*	10.0	(1.1–92.1)*	7.0	(2.0–24.6)***
Gray matter	14	0.9	(0.2–3.7)	1.6	(0.5–5.2)	0.9	(0.3–3.4)	0.5	(0.7–4.7)	1.4	(0.2–8.0)	1.8	(0.3–10.7)	1.0	(0.3–3.4)
White matter signal intensity															
DEHSI on T2–weighted imaging	10	1.5	(0.3–6.9)	0.9	(0.2–3.7)	1.7	(0.4–7.0)	0.8	(0.1–7.6)	0.8	(0.1–7.6)	1.0	(0.1–9.6)	2.0	(0.5–8.6)
FLAIR imaging	44	6.3	(0.8–52.7)	1.8	(0.6–6.2)	4.0	(0.8–19.9)		a		a	1.9	(0.2–17.9)	2.0	(0.6–6.5)
Multivariate analysis															
Adjusted for abnormal MRI findings															
Composite assessment															
White matter	23	6.2	(1.5–25.1)*	6.0	(1.7–20.9)**	6.3	(1.7–23.4)**		b		b		b	5.9	(1.6–22.2)**
Gray matter	14	0.7	(0.2–3.3)	1.3	(0.4–4.9)	0.6	(0.2–2.8)		b		b		b	0.8	(0.2–3.1)
White matter signal intensity															
DEHSI on T2–weighted imaging	10	1.5	(0.3–7.1)	0.6	(0.1–2.8)	1.3	(0.3–6.2)		b		b		b	1.5	(0.3–7.3)
FLAIR imaging	44	10.4	(1.1–98.7)*	1.4	(0.4–5.1)	5.6	(0.9–34.6)		b		b		b	1.6	(0.5–5.7)

Values are shown as the number of corresponding subjects or mean (95% CI). P values (*P < .05, **P < .01, and ***P < .005) are from logistic regression analysis. Analysis was not conducted for verbal IQ <70 because of insufficient corresponding subjects.

a Analysis was not conducted because of the complete separation of subjects.

b Analysis was not performed because of insufficient corresponding subjects.

TABLE 7 Sensitivity, Specificity, and Positive Likelihood Ratio of Composite Assessment on MRI in Predicting Cognitive Impairment at 9 Years Old

| | | Abnormal Findings on Composite Assessment | | | | | | Abnormal White Matter Signal Intensity | | | | | |
| | | White Matter | | | Gray Matter | | | DEHSI on T2-Weighted Imaging | | | FLAIR Imaging | | |
		Sens (%)	Spec (%)	LR+	Sens (%)	Spec (%)	LR+	Sens (%)	Spec(%)	LR+	Sens (%)	Spec (%)	LR+
Cognitive impairment													
Verbal IQ <85	Value	71	72	2.5	21	76	0.9	21	85	1.4	93	33	1.4
	95% CI	45–88	57–83	1.4–4.5	8–48	62–86	0.3–2.8	8–48	72–92	0.4–4.7	69–99	21–47	1.1–1.8
Performance IQ <85	Value	64	80	3.2	28	80	1.4	16	83	0.9	80	31	1.2
	95% CI	45–80	64–90	1.6–6.6	14–48	64–90	0.6–3.5	6–35	67–92	0.3–3.0	61–91	19–48	0.9–1.6
Full-scale IQ <85	Value	72	76	3.0	22	76	0.9	22	86	1.6	89	33	1.3
	95% CI	49–88	61–87	1.6–5.6	9–45	61–87	0.3–2.6	9–45	72–93	0.5–4.9	67–97	21–48	1.0–1.7
Verbal IQ <70	Value	100	64	2.8	50	78	2.2	0	83	0	100	28	1.4
	95% CI	34–100	51–75	2.0–3.9	9–91	65–86	0.5–9.7	0–66	71–90	NA	34–100	18–40	1.2–1.6
Performance IQ <70	Value	86	68	2.7	14	75	0.6	14	83	0.8	100	30	1.4
	95% CI	49–97	54–79	1.6–4.4	3–51	62–85	0.1–3.8	3–51	71–91	0.1–5.7	65–100	20–44	1.2–1.7
Full-scale IQ <70	Value	86	68	2.7	29	77	1.3	14	83	0.8	100	30	1.4
	95% CI	49–97	54–79	1.6–4.4	8–64	64–87	0.4–4.5	3–51	71–91	0.1–5.7	65–100	20–44	1.2–1.7
Cerebral palsy	Value	83	67	2.5	33	78	1.5	17	83	1.0	83	28	1.2
	95% CI	44–97	53–78	1.5–4.2	10–70	65–87	0.4–5.2	3–56	71–91	0.2–6.6	44–97	18–41	0.8–1.7
Special assistance	Value	56	85	3.6	24	77	1.0	21	88	17	79	35	12
	95% CI	39–71	66–94	1.4–9.4	12–40	58–89	0.4–2.6	10–37	71–96	0.5–6.2	63–90	19–54	0.9–1.7

LR+, likelihood ratio for a positive finding; NA, not applicable: CI not calculated because of the null sensitivity; Sens, sensitivity; Spec, specificity.

family environment compared with white matter injury.

Thus far, gray matter injury has been predominantly linked with cerebral injury for term-born infants, whereas white matter injury has been recognized as a prominent injury form for very preterm born infants.[2] However, recent studies highlighted that white matter injury and gray matter injury may coexist in both preterm and term subjects.[32,34,35] Studies in preterm infants suggest an association between gray matter abnormalities and moderate to severe (but not mild) white matter abnormalities[15,22]; the lack of correlations between gray matter injury and cognitive outcomes in our cohort may be in part caused by the difficulty in identifying subtle gray matter injury at term because of insufficient cortical gray matter volume.

Strengths and Limitations

To our knowledge, this is the first longitudinal study to compare term MRI findings with neurodevelopmental outcomes at middle school age. However,

given the dramatic alteration of higher cognitive functions after school age, additional studies with longer follow-up periods are necessary. The follow-up rate of our study would be acceptable for the period of 9 years; the cohort size was medium; however, it was still too small to incorporate sufficient number of clinical variables within the multivariate model; several important cofactors, such as maternal educational level and socioeconomic status, were unavailable.

MRI was obtained by using a relatively low magnetic field, which provided brain images with lower resolutions and thicker slices compared with those obtained by modern scanners. Our current study used qualitative assessment of term MRI as an established predictor of neurodevelopmental outcomes at 2 to 4 years old[15,16,36]; the evaluation of MRI might be slightly different from other institutions; assessments using quantitative MRI, such as apparent diffusion coefficient and fractional anisotropy, may provide additional diagnostic value. We used Wechsler Intelligence Scale for Children, Third Edition as the cognitive battery, which has

also been standardized for Japanese children; we were unable to assess the motor function.

Selection biases, including background characteristics of the unit and patients' clinical conditions, were not completely eliminated; indeed, the infants with intrauteral growth restriction were more likely to undergo MRI after 42 weeks corrected age; of the 16 infants who were lost to follow-up, only 1 and 2 infants showed abnormal white matter and gray matter abnormalities, respectively, based on the composite assessment. These limitations should be considered when interpreting our findings.

CONCLUSIONS

Our findings build on previous reports observing that very preterm born children are more likely to suffer a range of neurodevelopmental impairments compared with their peers. Consistent relationships between white matter injury at term and altered cognitive functioning at 9 years old were observed. Because ultrasound scans are insensitive to most MRI findings,[15,37]